The Multimessenger Chakra of Blazar Jets
Proceedings IAU Symposium No. 375, 2023
I. Liodakis, M. F. Aller, H. Krawczynski, A. Lähteenmäki & T. J. Pearson, eds.
doi:10.1017/S1743921323000881

Scientific Potential of MeV Polarimetry for Relativistic Jets

Haocheng Zhang

NASA Postdoc Program Fellow haocheng.zhang@nasa.gov
NASA Goddard Space Flight Center, Greenbelt, MD 20771, USA

Abstract. Relativistic jets from supermassive black holes or stellar mass black holes are among the most powerful astrophysical phenomena. Magnetic field plays an important role in the jet launching and propagation, as well as particle acceleration and radiation. Polarimetry is the only way to observe the magnetic field evolution. The recent launch of the Imaging X-ray Polarimetry Explorer (IXPE) has opened up the X-ray polarization window, which has revealed very interesting phenomena for relativistic jets. However, the field of MeV gamma-ray polarimetry remains largely unexplored. This paper aims to summarize key scientific potentials for MeV polarimetry for blazars and gamma-ray bursts (GRBs) from recent theoretical modeling. These predictions, which are closely related to the cosmic ray acceleration, neutrino production, radiation mechanism, and the jet evolution, can be examined by future MeV polarimeters, such as the Compton Spectrometer and Imager (COSI), the LargE Area burst Polarimeter (LEAP), and the All-sky Medium-Energy Gamma-ray Observatory eXplorer (AMEGO-X).

Keywords. polarimetry, blazar, gamma-ray burst

1. Introduction

Relativistic jets are highly energetic plasma outflows from accreting black holes. If the jet points very close to our line of sight, its apparent luminosity is boosted by the relativistic beaming effects. As a result, blazars, jets from supermassive black holes, and GRBs, jets from stellar mass black holes, are among the most powerful extragalactic γ-ray sources detected by *Fermi* (Abdollahi et al. 2020). Both blazars and GRBs are highly variable multi-wavelength sources, indicating extreme particle acceleration in the jet.

The highly variable multi-wavelength blazar emission shows a characteristic two-component spectrum. The low-energy spectral component extends from radio to optical bands, in some cases up to soft X-rays, while the high-energy component covers the X-ray and γ-ray bands. The low-energy component is dominated by the synchrotron emission from nonthermal electrons, evident by the observed high radio and optical polarization degree (for a recent review, see Zhang 2019), thus it is often referred to as the synchrotron component. Depending on the spectral peak of this component, blazars can be classified as the low-synchrotron-peaked (LSP), whose synchrotron peak is in the infrared bands, intermediate-synchrotron peaked (ISP), whose peak is in the optical to ultraviolet bands, and high-synchrotron-peaked (HSP), which peaks in the soft X-rays (Abdo et al. 2010). Observations have found that the location of the synchrotron peak is correlated to other observational properties such as the blazar luminosity and the spectral hardness (e.g., Ajello et al. 2020). This correlation is often referred to as the "blazar sequence". The origin of the high-energy component is still under debate. Many theoretical models suggest that the high-energy component results from the inverse Compton scattering of low-energy photons by the same nonthermal electron population that produces the

synchrotron component (Dermer et al. 1992; Ghisellini & Madau 1996; Maraschi et al. 1992; Marscher & Gear 1985; Sikora et al. 1994). The seed photons for Compton scattering can be the synchrotron emission itself, called the synchrotron self Compton (SSC), or the external thermal photons from the accretion disk, broad line region, molecular cloud, and/or the dusty torus, which is referred to as the external Compton (EC). This leptonic scenario is supported by the frequently observed simultaneous flaring of the synchrotron and high-energy components. On the other hand, the hadronic scenario argues that the blazar jet is sufficiently powerful to accelerate very high energy protons, which can produce the high-energy component via proton synchrotron and/or hadronic cascades (Aharonian 2000; Mannheim 1993; Mücke et al. 2003). Under this scenario, blazars are the extragalactic origin of cosmic rays and neutrinos (Böttcher et al. 2013; Cerruti et al. 2015). Recently, the *IceCube* detection of a very high energy neutrino in coincidence with the blazar TXS 0506+056 flare provides the first evidence for the hadronic scenario (IceCube Collaboration et al. 2018). However, detection of extragalactic neutrinos is very hard, and the leptonic and hadronic models generally produce similar multi-wavelength spectra, requiring additional observable signatures to distinguish between the two models (Chen et al. 2014; Diltz et al. 2015; Li & Kusunose 2000; Petropoulou et al. 2015; Sahu et al. 2013, and see Böttcher (2019) for a recent review).

GRBs consists of long bursts (more than two seconds) and short bursts (less than two seconds). Their origins are generally believed to be different: the former is probably due to the collapse of massive stars, while the latter results from the merger of binary neutron stars (Abbott et al. 2017; Goldstein et al. 2017; Hjorth et al. 2003; MacFadyen et al. 2001). For either long or short bursts, the prompt phase of the GRB is followed by the afterglow, which is due to the synchrotron emission in an optically thin environment. The prompt phase spectrum can be described by the Band function, but the underlying radiation mechanism is not well understood. Both the photospheric radiation and synchrotron emission in an optically thin environment are considered. In the photospheric model, photons are emitted inside the jet and keep interacting with the jet materials until they finally escape when the optical depth $\tau \sim 1$ (Beloborodov 2010; Pe'er et al. 2006; Rees & Mészáros 2005). In the synchrotron model, theoretical models such as the internal-collision-induced magnetic reconnection and turbulence (ICMART) model and the striped jet model often consider that the prompt emission region is magnetized, and the nonthermal particles are accelerated via magnetic reconnection and/or turbulence (Giannios & Uzdensky 2019; Rees & Meszaros 1994; Zhang & Yan 2011). The magnetic field in the prompt emission region may be ordered or disordered under the synchrotron model (Toma et al. 2009; Zhang & Yan 2011). Similar to the blazar γ-ray models, both the photospheric and synchrotron models can describe the GRB prompt emission spectra and light curves reasonably, requiring additional constraints to distinguish the two models.

This paper presents a review on the scientific potentials of MeV polarimetry for blazars and GRBs. For both systems, MeV polarimetry can diagnose the radiation mechanism of the γ-ray emission. MeV polarization degree that is comparable to or higher than the optical counterpart in blazars is an unambiguous evidence for the hadronic model, which can constrain the neutrino production and maximal cosmic ray energy obtainable in the blazar emission region. Additionally, the MeV polarization degree does not vary quickly due to the slow cooling of protons, ideal for detection by future MeV polarimeters. On the other hand, while a high MeV polarization degree prefers synchrotron emission in an ordered magnetic field for GRBs, the photospheric model cannot be ruled out. Time-dependent MeV polarization degree and angle variations are necessary to fully distinguish the physical mechanism for the GRB prompt emission.

https://doi.org/10.1017/S1743921323000881 Published online by Cambridge University Press

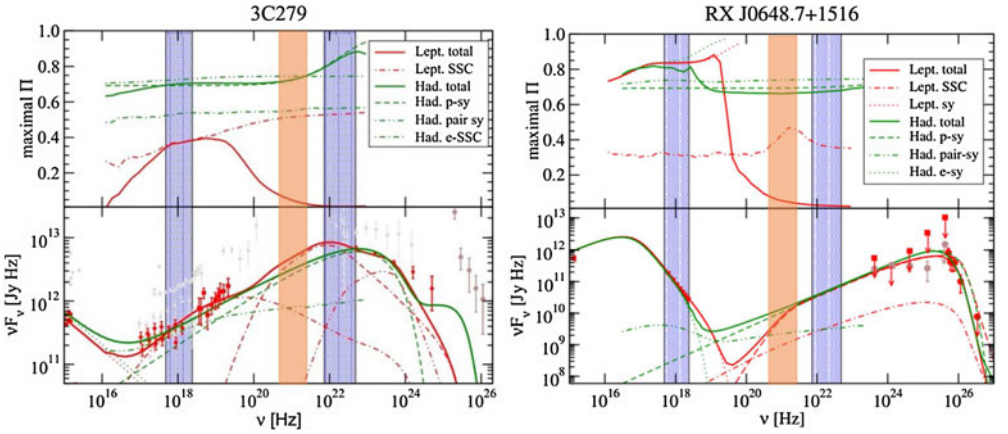

Figure 1. Multi-wavelength maximal polarization degree (upper panels) and spectral energy distribution (lower panels) for the two blazars 3C279 (left) and RX J0648.7+1516 (right). Leptonic model fits are plotted in red, hadronic models in green. Solid lines represent the model total, while other line styles indicate individual radiation components, as labeled in the legend. The orange shaded region represents the MeV band, while the blue shaded region on the left is approximately the *IXPE* soft X-ray band. This figure is reproduced from Zhang & Böttcher (2013).

2. Probe Blazar Cosmic Rays and Neutrinos with MeV Polarimetry

Neutrinos are obviously the smoking gun of the hadronic processes in blazar jets, as shown by the recent *IceCube* event (IceCube Collaboration et al. 2018). However, current neutrino detectors such as *IceCube* obtain adequately high statistics for neutrino detection. Additionally, the angular resolution is not very good, making it hard to determine the origin of the neutrinos. Given that neutrinos can travel through the universe without significant interaction with other materials, it is ambiguous to show whether neutrinos really come from a specific flaring blazar, even if the two events are simultaneous. MeV polarimetry provides a novel way to probe hadronic processes in blazars by identifying the radiation mechanisms. Aforementioned, the high-energy blazar spectral component in the hadronic model is dominated by the synchrotron emission from either protons or secondary charged particles produced by the hadronic cascades. The synchrotron emission is characterized by high polarization. In a perfectly ordered magnetic field, synchrotron emission can reach $\gtrsim 70\%$ polarization degree, depending on the spectral index (see Rybicki & Lightman 1986, for a detailed derivation). On the other hand, the inverse Compton scattering, which dominates the high-energy spectral component under the leptonic model, has relatively low polarization. Bonometto et al. (1970); Bonometto & Saggion (1973) have shown that isotropic inverse Compton scattering roughly reduces by half the polarization of the seed photons. In the case of SSC, where the seed photons come from synchrotron, the polarization degree after scattering is $\sim 40\%$; EC is unpolarized since the seed photons are unpolarized thermal photons. The above results have been confirmed by Krawczynski (2012) via Monte Carlo simulations. Based on the model in Bonometto et al. (1970), Zhang & Böttcher (2013) presents the first high-energy polarization prediction for LSP, ISP, and HSP blazars based on stationary blazar spectral fittings. As shown in Figure 1, the MeV polarization degree of the hadronic model is consistently higher than that of the leptonic model. While the X-ray polarization degree is also different for the leptonic and hadronic models, the X-ray emission may be contaminated by the low-energy synchrotron component, especially for the ISP and HSP blazars. Therefore, MeV polarimetry is ideal to distinguish the two models

https://doi.org/10.1017/S1743921323000881 Published online by Cambridge University Press

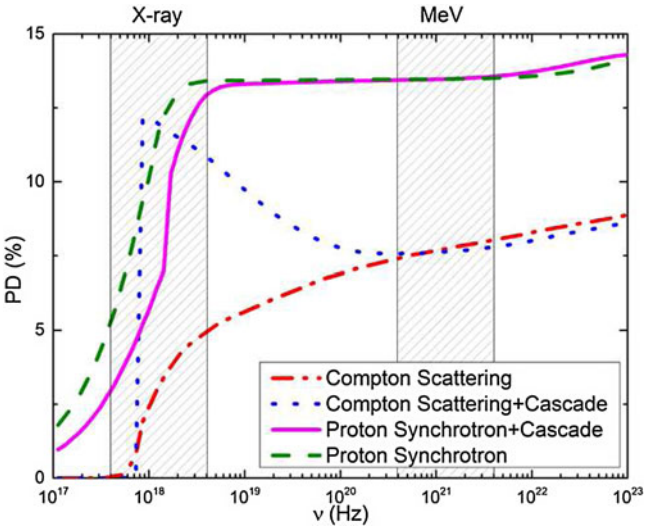

Figure 2. The X-ray to γ-ray spectral polarization degree based on the four leptonic and hadronic spectral fittings of the TXS 0506+056 neutrino event. The shaded regions correspond to the X-ray and MeV γ-ray bands. This figure is reproduced from Zhang et al. (2019).

for all blazar types. A key advantage of MeV polarimetry over the neutrino detection is that polarization is an intrinsic feature of photons, thus there is no ambiguity in whether the detected polarization is co-spatial with the emission.

Nonetheless, the above prediction is based on perfectly ordered magnetic fields. Optical polarization monitoring has matured in the last decade, showing typically $\lesssim 20\%$ polarization degree (Aliu et al. 2016; Blinov et al. 2018; Larionov et al. 2013; Marscher et al. 2010; Morozova et al. 2014). This implies a partially ordered magnetic field in the blazar emission region (Pushkarev et al. 2005; Zhang et al. 2015). If the low- and high-energy spectral components are co-spatial, the high-energy emission should suffer from the same depolarization effect due to partially ordered magnetic field as the low-energy emission. This depolarization factor can be estimated by the ratio of the observed optical polarization degree over the maximal synchrotron polarization degree in a perfectly ordered magnetic field by modeling the low-energy spectral index. However, many LSP blazars, especially flat spectrum radio quasars, have a strong thermal emission component in the optical band. In these sources, the optical polarization can be contaminated by the unpolarized thermal emission. Therefore, the depolarization factor should be calculated by first removing the thermal contamination. Paliya et al. (2018) has performed the above calculation and found that the hadronic model typically predicts comparable or higher MeV polarization degree than the optical band, while the leptonic model generally predicts less than half of the optical polarization. More recently, Zhang et al. (2019) have performed a detailed X-ray and MeV polarization prediction for the TXS 0506+056 flare and neutrino event. By comparing different spectral fitting models, this paper suggests that while X-ray and MeV polarization can both probe hadronic processes for TXS 0506+056, MeV polarimetry is unique in identifying the proton synchrotron process (see Figure 2. Since the proton synchrotron is only efficient in a strong magnetic field, preventing significant contributions from inverse Compton scattering, the γ-ray emission is dominated by the proton synchrotron. Spectral fittings then suggest that the observed γ-ray emission is produced by nonthermal protons extending to $\sim$EeV, i.e., the blazar emission region can

https://doi.org/10.1017/S1743921323000881 Published online by Cambridge University Press

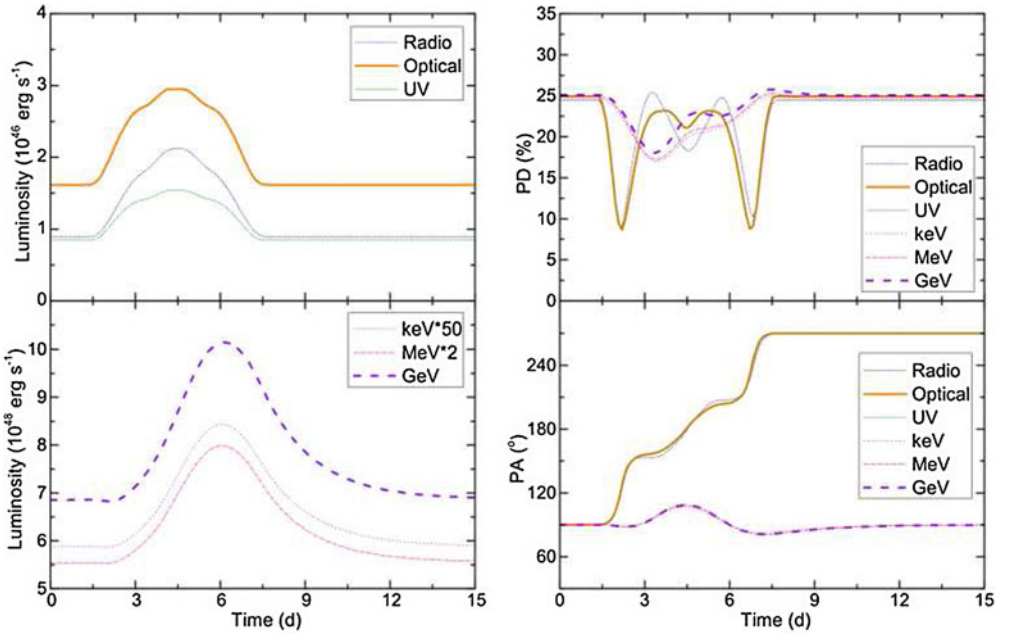

Figure 3. Light curves and polarization variations for the hadronic model. Left: multiwavelength light curves chosen at radio (30–300 GHz, navy short-dashed), optical (1.8–3.2 eV, thick orange solid), UV (3.3–6.2 eV, olive dot-dot-dashed), X-ray (60–200 keV, purple dotted), MeV γ-ray (5–200 MeV, AdEPT, pink dot-dashed), and GeV γ-ray (20 MeV–300 GeV, Fermi-LAT, thick violet dashed) bands. Due to the large bandwidth of the GeV light curve, it collects a much higher total luminosity than the keV and MeV bands. Hence, we manually boost those two bands by a fixed number to allow us to show them in the same figure. Right: multiwavelength PD and PA vs. time. Bands are chosen the same as light curves. This figure is reproduced from Zhang et al. (2016).

accelerate ultra-high-energy cosmic rays (UHECRs) (Böttcher et al. 2013; Cerruti et al. 2015). This study, although using rather simplified spectral fitting models, shows the potential that MeV polarimetry can explore the acceleration of UHECRs in blazars.

A major concern of detecting blazar MeV polarization is the variability. It is known that the blazar optical polarization can change, including large polarization angle swings (Blinov et al. 2015, 2018; Jorstad et al. 2022; Marscher et al. 2010). Since the MeV polarimeters cannot achieve the same temporal resolution as the optical counterparts due to the very low number of photons, they will require much longer time to integrate enough photons to determine the MeV polarization degree. If the polarization angle rotates significantly during this time window, the net polarization degree will drop. Zhang et al. (2016) has studied this issue with a multi-zone time-dependent simulation. Fortunately, the MeV polarization degree and angle are unlikely to change considerably during flares, due to the very slow proton cooling. In a typical blazar emission region, the proton cooling time scale is usually longer than the light crossing time scale, the latter is generally comparable to the time scale of magnetic field evolution either due to shocks or magnetic instabilities. On the other hand, electrons can quickly react to changes in the magnetic field, due to their very fast cooling. Zhang et al. (2016) considers a simulation setup with a major magnetic field morphology change in the blazar emission region, which drives a large polarization angle swing in the low-energy bands as shown in Figure 3. However, protons only slowly react to the changes due to their long cooling time, leading to a small dip in the polarization degree and minor fluctuations in the polarization angle,

https://doi.org/10.1017/S1743921323000881 Published online by Cambridge University Press

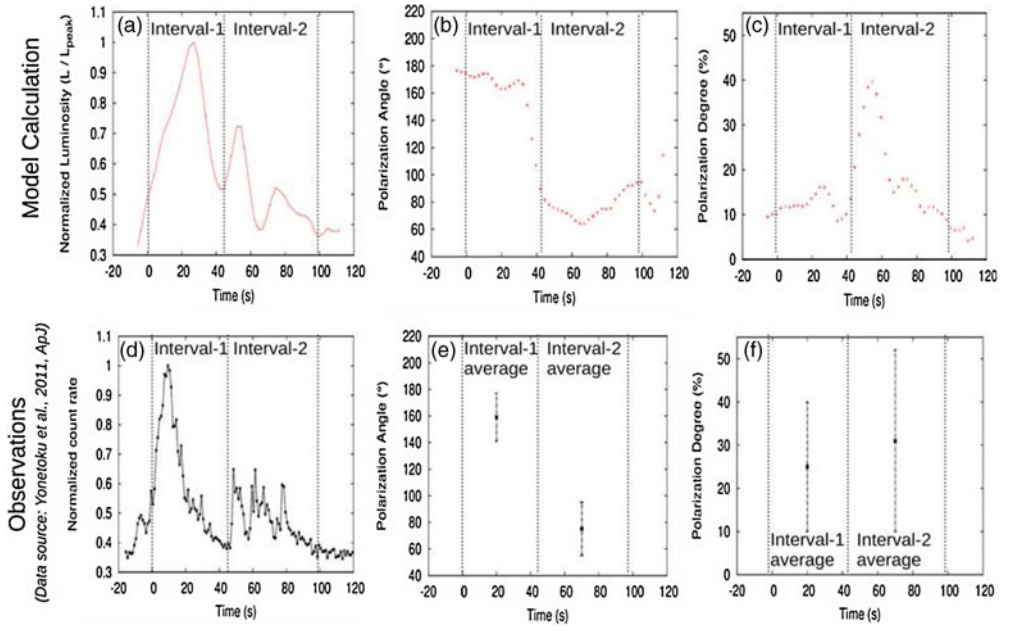

Figure 4. Comparison between integrated magnetohydrodynamic and polarized radiation transfer simulation results and GRB 100826A observation. Upper panels are the light curve as well as polarization angle and degree from the simulation, whereas the lower panels are the observation by Yonetoku et al. (2011). The light curves of both observation and calculation are normalized by their peak values. This figure is reproduced from Deng et al. (2016).

ideal for future MeV polarimeters to integrate a relatively long time for polarization detection. On the other hand, the leptonic scenario suffers from double depolarization due to partially ordered magnetic field. This is because the seed photons for SSC observe a partially ordered magnetic field thus get depolarized, while SSC from different parts of the emission region shall have their seed photons with different polarization status, resulting in a second depolarization. If the magnetic field can vary, the light crossing delay will cause the seed photons and the scattered photons arriving at different time, overall enhancing this double depolarization effect. This has been studied in Peirson et al. (2022), showing that the leptonic polarization degree is $\lesssim 30\%$ of the optical counterpart, almost impossible for future MeV polarimetry. Therefore, a detection of MeV polarization during blazar flares is almost certainly a signature of hadronic processes.

3. Understand GRB Prompt Emission with MeV Polarimetry

Similar to blazars, MeV polarimetry can also study the GRB prompt emission mechanisms. The synchrotron model clearly expects to have some level of γ-ray polarization, whether the magnetic field is ordered or disordered, although the former case predicts much higher polarization degree. Photons in the photospheric model experience scattering in the emission region before they can escape. However, unlike blazars, the scattering in GRBs is anisotropic, thus the resulting polarization degree can range from 0 to nearly 100%, depending on the viewing angle. Toma et al. (2009) presents a pioneering work on the GRB prompt polarization, in which they find an interesting distribution of prompt polarization degrees based on different models. This paper points to the potential of studying GRB prompt polarization statistically with a large number of accurate measurement to distinguish different models. A major issue here is that it is unlikely that all GRBs belong to one particular kind of prompt emission models. Current prompt

https://doi.org/10.1017/S1743921323000881 Published online by Cambridge University Press

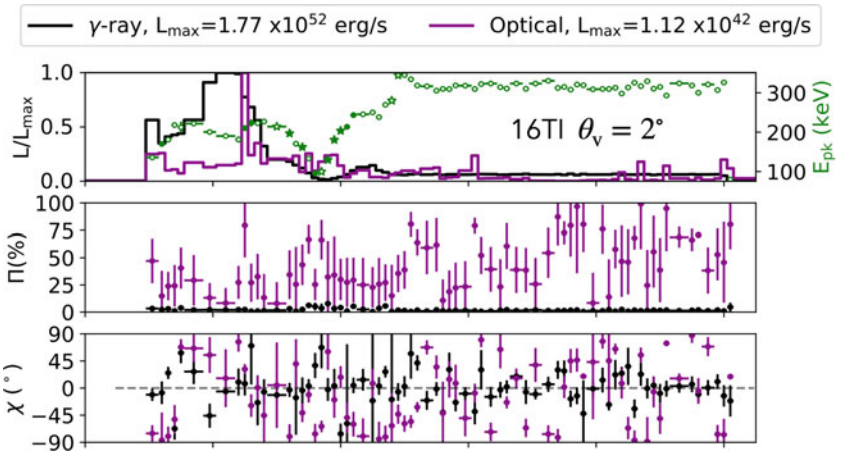

Figure 5. Light curve and polarization from integrated hydrodynamic and polarized radiation transfer simulations. The upper panel plots the time-resolved fitted spectral peak energy E_{pk} in green and the γ-ray and optical light curves in black and magenta respectively, where each light curve is normalized by its own maximum value. The middle panel plots the polarization degree of the γ-ray and optical photons in black and magenta. The lower panel shows the polarization angles of the mock observed γ-ray and optical bands. This figure is reproduced from Parsotan & Lazzati (2022).

polarization measurements, though with large error bars, do not show clear trends in the polarization degree distributions. Recently, Gill et al. (2020) present a more detailed study, but they still reach the conclusion that the synchrotron and photospheric models tend to have similar distributions of prompt polarization degrees. Their paper does argue that very high polarization ($\gtrsim 50\%$) is more naturally produced by the synchrotron model under typical jet configurations, but since the GRB jet morphology and physical conditions are not well understood either, collection of average prompt polarization degrees from many GRBs is insufficient to diagnose the GRB radiation mechanisms.

Temporally resolved prompt polarization degree and angle evolution are crucial to explore the GRB radiation. Based on the ICMART model, Deng et al. (2016) presents a pioneering numerical study of the prompt radiation and polarization signatures (see Figure 4. They employ integrated magnetohydrodynamic and polarized radiation transfer simulations to study the light curve and time-dependent polarization degree and angle from magnetic reconnection. This approach can self-consistently track the magnetic field structure and evolution so as to self-consistently derive polarization signatures. Very interestingly, they find a strong change of polarization degree and a $\sim 90^\circ$ angle swing happening between two peaks in the prompt light curve, well resembling the observation presented in Yonetoku et al. (2011). We note that the polarization angle swing is not limited to 90° in the magnetic reconnection scenario. As demonstrated in recent integrated particle-in-cell and polarized radiation transfer simulations, reconnection can result in large angle swings that are accompanied by changes in polarization degree and flares (Zhang et al. 2021, 2022). Using a semi-analytical model, Gill & Granot (2021) draw similar conclusions in a recent paper, where they explore time-dependent polarization from more general synchrotron models with various magnetic field configurations (see Figure 5). For the photospheric model, Parsotan & Lazzati (2022) calculates the time-dependent polarization based on integrated hydrodynamic and polarized radiation transfer simulations, in which they also find a 90° polarization angle swing. Given the nature of photon scattering in the photospheric model, γ-ray polarization results from anisotropic scattering, thus the polarization degree and angle are closely related as shown

https://doi.org/10.1017/S1743921323000881 Published online by Cambridge University Press

in Parsotan & Lazzati (2022). Such correlation is not present in the synchrotron model. Additionally, the amplitude of continuous angle rotation is limited to 90° in the photospheric model, while the amplitude in a synchrotron model is arbitrary, at least based on a magnetic reconnection scenario.

4. Future Prospects

Future MeV polarimeters may examine the above theoretical predictions for blazars and GRBs. POLAR-2 is a planned γ-ray polarimeter for GRBs, which is projected to measure about 50 GRBs per year with equal or better quality compared to the best seen by POLAR (Hulsman 2020). Recently, NASA selected LEAP as a Mission of Opportunity, which is an MeV polarimeter that may be deployed on the International Space Station (McConnell et al. 2021). Both POLAR-2 and LEAP may have the capability to resolve time-dependent GRB polarization for very bright GRBs. However, they are not designed to observed persistent sources like blazars. COSI is a selected SMEX mission that can detect γ-ray polarization for both blazars and GRBs (Yang et al. 2018). Its sensitivity may be able to detect a couple of hadronic blazar polarization signatures during its mission span if they exhibit bright flares. AMEGO-X is a more powerful MeV polarimeter that is under development (Caputo et al. 2022). It may detect polarization from ten bright blazar flares per year if they are hadronic, more conclusively distinguishing the leptonic and hadronic blazar models. These missions can complement the ongoing X-ray polarimeter IXPE to cover the high-energy polarimetry for relativistic jets.

Theoretically, previous works have already demonstrated the importance of numerical simulations. With the development of more efficient numerical codes and connection between particle acceleration, fluid dynamics, and radiation transfer, future simulations are expected to link the kinetic scale of particles with the large-scale fluid dynamics to fully study radiation and polarization signatures under realistic blazar and GRB physical conditions. MeV polarimetry can become a key component of the multi-messenger astronomy in the next decade.

References

Abbott, B. P., Abbott, R., Abbott, T. D., et al. 2017, ApJ, 848, L13. doi:10.3847/2041-8213/aa920c

Abdo, A. A., Ackermann, M., Agudo, I., et al. 2010, ApJ, 716, 30. doi:10.1088/0004-637X/716/1/30

Abdollahi, S., Acero, F., Ackermann, M., et al. 2020, ApJS, 247, 33. doi:10.3847/1538-4365/ab6bcb

Aharonian, F. A. 2000, New Astron., 5, 377. doi:10.1016/S1384-1076(00)00039-7

Ajello, M., Angioni, R., Axelsson, M., et al. 2020, ApJ, 892, 105. doi:10.3847/1538-4357/ab791e

Aliu, E., Archambault, S., Archer, A., et al. 2016, A&A, 594, A76. doi:10.1051/0004-6361/201628744

Beloborodov, A. M. 2010, MNRAS, 407, 1033. doi:10.1111/j.1365-2966.2010.16770.x

Blinov, D., Pavlidou, V., Papadakis, I., et al. 2015, MNRAS, 453, 1669. doi:10.1093/mnras/stv1723

Blinov, D., Pavlidou, V., Papadakis, I., et al. 2018, MNRAS, 474, 1296. doi:10.1093/mnras/stx2786

Bonometto, S., Cazzola, P., & Saggion, A. 1970, A&A, 7, 292

Bonometto, S. & Saggion, A. 1973, A&A, 23, 9

Böttcher, M., Reimer, A., Sweeney, K., et al. 2013, ApJ, 768, 54. doi:10.1088/0004-637X/768/1/54

Böttcher, M. 2019, Galaxies, 7, 20. doi:10.3390/galaxies7010020

Caputo, R., Ajello, M., Kierans, C. A., et al. 2022, Journal of Astronomical Telescopes, Instruments, and Systems, 8, 044003. doi:10.1117/1.JATIS.8.4.044003
Cerruti, M., Zech, A., Boisson, C., et al. 2015, MNRAS, 448, 910. doi:10.1093/mnras/stu2691
Chen, X., Chatterjee, R., Zhang, H., et al. 2014, MNRAS, 441, 2188. doi:10.1093/mnras/stu713
Deng, W., Zhang, H., Zhang, B., et al. 2016, ApJ, 821, L12. doi:10.3847/2041-8205/821/1/L12
Dermer, C. D., Schlickeiser, R., & Mastichiadis, A. 1992, A&A, 256, L27
Diltz, C., Böttcher, M., & Fossati, G. 2015, ApJ, 802, 133. doi:10.1088/0004-637X/802/2/133
Ghisellini, G. & Madau, P. 1996, MNRAS, 280, 67. doi:10.1093/mnras/280.1.67
Giannios, D. & Uzdensky, D. A. 2019, MNRAS, 484, 1378. doi:10.1093/mnras/stz082
Gill, R., Granot, J., & Kumar, P. 2020, MNRAS, 491, 3343. doi:10.1093/mnras/stz2976
Gill, R. & Granot, J. 2021, MNRAS, 504, 1939. doi:10.1093/mnras/stab1013
Goldstein, A., Veres, P., Burns, E., et al. 2017, ApJ, 848, L14. doi:10.3847/2041-8213/aa8f41
Hjorth, J., Sollerman, J., Møller, P., et al. 2003, Nature, 423, 847. doi:10.1038/nature01750
Hulsman, J. 2020, Proc. SPIE, 11444, 114442V. doi:10.1117/12.2559374
IceCube Collaboration, Aartsen, M. G., Ackermann, M., et al. 2018, Science, 361, eaat1378. doi:10.1126/science.aat1378
Jorstad, S. G., Marscher, A. P., Raiteri, C. M., et al. 2022, Nature, 609, 265. doi:10.1038/s41586-022-05038-9
Krawczynski, H. 2012, ApJ, 744, 30. doi:10.1088/0004-637X/744/1/30
Larionov, V. M., Jorstad, S. G., Marscher, A. P., et al. 2013, ApJ, 768, 40. doi:10.1088/0004-637X/768/1/40
Li, H. & Kusunose, M. 2000, ApJ, 536, 729. doi:10.1086/308960
MacFadyen, A. I., Woosley, S. E., & Heger, A. 2001, ApJ, 550, 410. doi:10.1086/319698
Mannheim, K. 1993, A&A, 269, 67. doi:10.48550/arXiv.astro-ph/9302006
Maraschi, L., Ghisellini, G., & Celotti, A. 1992, ApJ, 397, L5. doi:10.1086/186531
Marscher, A. P. & Gear, W. K. 1985, ApJ, 298, 114. doi:10.1086/163592
Marscher, A. P., Jorstad, S. G., Larionov, V. M., et al. 2010, ApJ, 710, L126. doi:10.1088/2041-8205/710/2/L126
Morozova, D. A., Larionov, V. M., Troitsky, I. S., et al. 2014, AJ, 148, 42. doi:10.1088/0004-6256/148/3/42
McConnell, M. L., Baring, M., Bloser, P., et al. 2021, Proc. SPIE, 11821, 118210P. doi:10.1117/12.2594737
Mücke, A., Protheroe, R. J., Engel, R., et al. 2003, Astroparticle Physics, 18, 593. doi:10.1016/S0927-6505(02)00185-8
Paliya, V. S., Zhang, H., Böttcher, M., et al. 2018, ApJ, 863, 98. doi:10.3847/1538-4357/aad1f0
Parsotan, T. & Lazzati, D. 2022, ApJ, 926, 104. doi:10.3847/1538-4357/ac4093
Pe'er, A., Mészáros, P., & Rees, M. J. 2006, ApJ, 642, 995. doi:10.1086/501424
Peirson, A. L., Liodakis, I., & Romani, R. W. 2022, ApJ, 931, 59. doi:10.3847/1538-4357/ac6a54
Petropoulou, M., Dimitrakoudis, S., Padovani, P., et al. 2015, MNRAS, 448, 2412. doi:10.1093/mnras/stv179
Pushkarev, A. B., Gabuzda, D. C., Vetukhnovskaya, Y. N., et al. 2005, MNRAS, 356, 859. doi:10.1111/j.1365-2966.2004.08535.x
Rees, M. J. & Meszaros, P. 1994, ApJ, 430, L93. doi:10.1086/187446
Rees, M. J. & Mészáros, P. 2005, ApJ, 628, 847. doi:10.1086/430818
Rybicki, G. B. & Lightman, A. P. 1986, Radiative Processes in Astrophysics, by George B. Rybicki, Alan P. Lightman, pp. 400. ISBN 0-471-82759-2. Wiley-VCH, June 1986., 400
Sahu, S., Oliveros, A. F. O., & Sanabria, J. C. 2013, Phys. Rev. D, 87, 103015. doi:10.1103/PhysRevD.87.103015
Sikora, M., Begelman, M. C., & Rees, M. J. 1994, ApJ, 421, 153. doi:10.1086/173633
Toma, K., Sakamoto, T., Zhang, B., et al. 2009, ApJ, 698, 1042. doi:10.1088/0004-637X/698/2/1042

Yang, C.-Y., Lowell, A., Zoglauer, A., et al. 2018, Proc. SPIE, 10699, 106992K. doi:10.1117/12.2312556
Yonetoku, D., Murakami, T., Gunji, S., et al. 2011, ApJ, 743, L30. doi:10.1088/2041-8205/743/2/L30
Zhang, B. & Yan, H. 2011, ApJ, 726, 90. doi:10.1088/0004-637X/726/2/90
Zhang, H. & Böttcher, M. 2013, ApJ, 774, 18. doi:10.1088/0004-637X/774/1/18
Zhang, H., Chen, X., Böttcher, M., et al. 2015, ApJ, 804, 58. doi:10.1088/0004-637X/804/1/58
Zhang, H., Diltz, C., & Böttcher, M. 2016, ApJ, 829, 69. doi:10.3847/0004-637X/829/2/69
Zhang, H., Fang, K., Li, H., et al. 2019, ApJ, 876, 109. doi:10.3847/1538-4357/ab158d
Zhang, H. 2019, Galaxies, 7, 85. doi:10.3390/galaxies7040085
Zhang, H., Li, X., Giannios, D., et al. 2021, ApJ, 912, 129. doi:10.3847/1538-4357/abf2be
Zhang, H., Li, X., Giannios, D., et al. 2022, ApJ, 924, 90. doi:10.3847/1538-4357/ac3669